
Initial Results of a Prospective Clinical Trial of ^{18}F -Fluciclovine PET/CT in Newly Diagnosed Invasive Ductal and Invasive Lobular Breast Cancers

Gary A. Ulaner^{1,2}, Debra A. Goldman³, Mithat Gönen³, Hanh Pham¹, Raychel Castillo⁴, Serge K. Lyashchenko^{1,5}, Jason S. Lewis^{1,2,5,6}, and Chau Dang⁷

¹Department of Radiology, Memorial Sloan Kettering Cancer Center, New York, New York; ²Departments of Radiology and Pharmacology, Weill Cornell Medical College, New York, New York; ³Department of Epidemiology and Biostatistics, Memorial Sloan Kettering Cancer Center, New York, New York; ⁴Hunter College of the City College of New York, New York, New York; ⁵Radiochemistry & Molecular Imaging Probe Core, Memorial Sloan Kettering Cancer Center, New York, New York; ⁶Molecular Pharmacology Program, Memorial Sloan Kettering Cancer Center, New York, New York; and ⁷Department of Medicine, Memorial Sloan Kettering Cancer Center, New York, New York

^{18}F -labeled 1-amino-3-fluorocyclobutane-1-carboxylic acid (^{18}F -fluciclovine) is a leucine analog PET/CT radiotracer that depicts amino acid transport into cells. Amino acid transport proteins have been shown to be upregulated in breast malignancies by microarray and immunohistochemical analysis, so we hypothesized that ^{18}F -fluciclovine may provide a novel method of visualizing breast cancer and now report a prospective clinical trial of ^{18}F -fluciclovine PET/CT in newly diagnosed advanced local invasive ductal carcinoma (IDC) and invasive lobular carcinoma (ILC). **Methods:** Twenty-seven women with a new diagnosis of locally advanced IDC ($n = 19$) or ILC ($n = 8$) underwent PET/CT of the chest after intravenous administration of 370 MBq of ^{18}F -fluciclovine. The SUV_{max} , SUV_{mean} , metabolic tumor volume, and total lesion avidity were obtained for the primary breast tumor, axillary lymph nodes, and extraaxillary lymph nodes. Sites of previously unsuspected malignancy were recorded and confirmed by pathology. Results of ^{18}F -fluciclovine PET/CT were compared with those of ^{18}F -FDG PET/CT, when available, using the concordance correlation coefficient. **Results:** All locally advanced breast cancers were ^{18}F -fluciclovine-avid. Of 21 patients with pathologically proven axillary nodal metastases, ^{18}F -fluciclovine-avid axillary nodes were seen in 20. ^{18}F -fluciclovine detected pathologically proven extraaxillary nodal metastases in 3 patients, including 2 previously unsuspected internal mammary nodes. Fourteen patients underwent ^{18}F -FDG PET/CT for comparison with ^{18}F -fluciclovine. Concordance for metabolic tumor volume between ^{18}F -fluciclovine and ^{18}F -FDG was strong (concordance correlation coefficient, 0.89; 95% confidence interval, 0.73–0.96), but concordance for SUV_{max} was weak (concordance correlation coefficient, 0.04; 95% confidence interval, –0.16–0.24). In patients with both modalities available ($n = 14$), primary ILCs ($n = 4$) demonstrated ^{18}F -fluciclovine avidity (median SUV_{max} , 6.1; range, 4.5–10.9) greater than ^{18}F -FDG avidity (median SUV_{max} , 3.7; range, 1.8–6.0). Primary IDCs ($n = 10$) had a lower ^{18}F -fluciclovine avidity (median SUV_{max} , 6.8; range, 3.6–9.9) than ^{18}F -FDG avidity (median SUV_{max} , 10; range, 3.3–43.5). **Conclusion:** ^{18}F -fluciclovine PET/CT demonstrates potential for imaging of both IDC and ILC, including the detection of unsuspected extraaxillary nodal metastases. The low concordance for

SUV_{max} between ^{18}F -fluciclovine and ^{18}F -FDG suggests that these tracers measure different biologic phenomena within the tumor. The apparently higher uptake of ^{18}F -fluciclovine in ILC requires confirmation in a larger cohort.

Key Words: ^{18}F -fluciclovine; ^{18}F -FACBC; PET/CT; ductal; lobular; breast cancer

J Nucl Med 2016; 57:1350–1356

DOI: 10.2967/jnumed.115.170456

PET with ^{18}F -FDG has made important advances in the care of patients with breast cancer (1); however, ^{18}F -FDG PET has multiple limitations, including the inability to differentiate malignant from benign breast lesions (2), limited contribution to local staging of the breast and axillary nodes (3–5), and variable sensitivity for breast cancer depending on tumor and patient factors (6–8). Invasive lobular carcinoma (ILC), a subtype of breast cancer, is difficult to visualize by all known imaging modalities (9,10), including ^{18}F -FDG PET (11–16). Thus, there is a continued need for the development of better metabolic imaging agents for breast cancer, particularly for ILC.

Amino acid transport is highly upregulated in breast cancers as compared with normal breast epithelium by microarray and immunohistochemical analysis (17), suggesting that imaging agents for breast malignancies based on amino acid metabolism may be useful. ^{18}F -labeled 1-amino-3-fluorocyclobutane-1-carboxylic acid (^{18}F -fluciclovine, also known as ^{18}F -FACBC) is a leucine analog PET/CT radiotracer that depicts amino acid transport and is under investigation as a tumor-targeting agent (18–22). We hypothesized that the upregulation of genes for amino acid transport proteins in breast cancer will favor enhanced ^{18}F -fluciclovine uptake and allow for clinically valuable imaging in this tumor type. In this article, we report our initial results of ^{18}F -fluciclovine PET/CT from a prospective clinical trial of patients with the 2 most common subtypes of breast cancer, invasive ductal carcinoma (IDC), which accounts for approximately 75%–80% of primary breast malignancies, and ILC, which accounts for approximately 10%–15% (23).

Received Nov. 25, 2015; revision accepted Feb. 17, 2016.

For correspondence or reprints contact: Gary A. Ulaner, Department of Radiology, Memorial Sloan Kettering Cancer Center, 1275 York Ave., P.O. Box 77, New York, NY 10065.

E-mail: ulanerg@mskcc.org

Published online Mar. 3, 2016.

COPYRIGHT © 2016 by the Society of Nuclear Medicine and Molecular Imaging, Inc.

MATERIALS AND METHODS

Study Design and Patients

This prospective clinical trial was performed with institutional review board approval and written informed consent from participants. Patients presenting for evaluation at Memorial Sloan Kettering Cancer Center with biopsy-proven locally advanced, nonmetastatic, IDC or ILC who were referred for neoadjuvant systemic therapy between August 2013 and August 2015 were invited to participate. This patient population allows for an initial evaluation of ^{18}F -fluciclovine avidity in larger tumors. Exclusion criteria were age younger than 18 y, current pregnancy or lactation, prior malignancy other than squamous or basal skin cancers, and patients unwilling or unable to consent. There were no restrictions on sex or race. ILC patients were actively sought, which accounts for the higher prevalence of ILC in our cohort than in the overall breast cancer population. Clinical records were used to document patient age, sex, race, and presence of biopsy-proven known axillary or extraaxillary nodal metastases before ^{18}F -fluciclovine PET/CT as well as histology, grade, and receptor status of the primary breast malignancy. Tumors were hormone receptor–positive if they stained as estrogen receptor greater than 1% or progesterone receptor greater than 1%. Tumors were human epidermal growth factor receptor 2–positive if they were immunohistochemistry 3+ or fluorescent in situ hybridization amplified with ratio of $> / = 2.0$.

^{18}F -Fluciclovine Production

^{18}F -fluciclovine was manufactured in compliance with current good manufacturing practice requirements at the Memorial Sloan Kettering Cancer Center Radiochemistry and Molecular Imaging Probes Core Facility. The FASTlab automated synthesizer, synthesizer cassettes, reagents, and materials were all supplied by GE Healthcare as previously described (24). The automated synthesis involved nucleophilic incorporation of ^{18}F -fluoride into the ^{18}F -fluciclovine precursor, followed by removal of protective groups using hydrolysis and terminal sterilization with a 0.22- μm sterilizing filter. The ^{18}F -fluciclovine final drug product was formulated with 200 mM citrate buffer solution. All manufactured ^{18}F -fluciclovine drug product batches were quality control tested to ensure conformance with the acceptance specifications for pH, appearance, radiochemical purity, radiochemical identity, radionuclidic identity, endotoxin levels, sterilizing filter integrity, and residual solvent levels before release for patient administration.

^{18}F -Fluciclovine PET/CT Imaging and Image Interpretation

Enrolled patients underwent ^{18}F -fluciclovine PET/CT before initiation of therapy. There was no patient-specific preparation before ^{18}F -fluciclovine administration, and patients were allowed to eat and drink before the PET/CT examination, in contrast to previous work in prostate cancer (21). Patients were positioned on designated research PET/CT scanners, either a Discovery STE or a GE Discovery 710 (GE Healthcare), operated in 3-dimensional mode. The ^{18}F -fluciclovine PET studies were performed as hybrid PET/CT examinations for attenuation correction, lesion localization, and availability of additional CT data. A low-milliampere CT (60–80 mA) of the chest was acquired first. Then a bolus of 370 MBq (10 mCi) \pm 10% of ^{18}F -fluciclovine was administered intravenously in under 10 s. Dynamic PET imaging over the chest was acquired for 30 min, with data collected for each minute, then summed into 5-min intervals. ^{18}F -fluciclovine avidity was most often greatest during the 5- to 10-min time interval, and therefore quantitative analyses of ^{18}F -fluciclovine avidity were conducted using the data collected during this time interval. The ^{18}F -fluciclovine PET/CT images were reconstructed using iterative reconstruction and displayed on a PET/CT workstation (PET VCAR; GE Healthcare) in multiplanar reconstructions.

TABLE 1
Patient and Tumor Characteristics

Characteristic	n (%)
Sex	
Female	27 (100)
Race	
Caucasian	20 (74.1)
Black	4 (14.8)
Asian	1 (3.7)
Hispanic	2 (7.4)
Histology	
IDC	19 (70.4)
ILC	8 (29.6)
Histologic grade	
1	2 (7.4)
2	8 (29.6)
3	17 (63)
AJCC tumor stage*	
2B	13 (48.1)
3A	6 (22.2)
3B	6 (22.2)
3C	2 (7.4)
Receptor status	
ER or PR+/HER2–	13 (48.1)
HER2+	7 (25.9)
Triple negative (ER–/PR–/HER2–)	7 (25.9)

*Clinical classification according to seventh edition of the AJCC Staging Manual (26).

AJCC = American Joint Committee on Cancer; ER = estrogen receptor; PR = progesterone receptor; HER2 = human epidermal growth factor receptor 2.

Median age at diagnosis was 52.7 y (range, 37.3–79.1 y).

Areas of focal tracer uptake were localized using the companion CT and classified as lesions of the breast, axillary nodes, or extra-axillary lesions. Three-dimensional regions of interest were placed in areas of tracer uptake, and measures of ^{18}F -fluciclovine avidity were recorded, including SUV_{max} (body weight), metabolic tumor volume (MTV) (cubic centimeter volume of tumor with SUV greater than 42% of SUV_{max}), SUV_{mean} (within the MTV), and total lesion avidity ($\text{TLA} = \text{MTV} \times \text{SUV}_{\text{mean}}$).

Comparison ^{18}F -FDG PET/CT Imaging and Image Interpretation

Although not prescribed as part of the clinical trial, some patients underwent ^{18}F -FDG PET/CT as part of their standard clinical care before initiation of therapy. Patients fasted for at least 6 h before the ^{18}F -FDG PET/CT scan. Each patient was injected intravenously with 444 MBq (12 mCi) of ^{18}F -FDG when plasma glucose was less than 200 mg/dL. After ^{18}F -FDG injection, patients rested for a scheduled 60-min uptake period, followed by image acquisition. PET/CT scans were acquired with the patient supine from the base of the skull to the mid thigh. A low-dose CT scan with oral contrast was obtained. ^{18}F -FDG PET/CT images were reconstructed

TABLE 2

Measurements of ¹⁸F-Fluciclovine Avidity in Primary Breast Malignancies, Axillary Nodes, and Extraaxillary Nodes

Lesion site	Measurements of avidity	By histology								
		All patients (n = 27)			IDC (n = 19)			ILC (n = 8)		
		n	Median	Minimum to maximum	n	Median	Minimum to maximum	n	Median	Minimum to maximum
Breast malignancy	SUV _{max}	27	5.9	1.7–17.0	19	6.8	2.6–17.0	8	4.6	1.7–10.9
	SUV _{mean}		3.3	1.4–7.1		3.9	1.5–7.1		2.6	1.4–5.8
	MTV		16.1	3.2–102.0		15.3	3.2–74.6		32.6	3.6–102.0
	TLA		56.8	5.0–370.6		54.5	14.8–283.7		89.6	5.0–370.6
Axillary nodes	SUV _{max}	20	5.6	1.2–14.6	16	5.4	1.2–12.6	4	7.0	1.3–14.6
	SUV _{mean}		3.3	1.0–7.9		3.2	1.0–7.9		4.2	1.2–6.2
	MTV		4.4	1.0–22.1		4.9	1.0–13.4		3.2	1.1–22.1
	TLA		12.6	1.0–137.0		13.8	1.0–52.3		12.6	1.3–137.0
Extraaxillary nodes	SUV _{max}	3	2.6	2.2–4.2	3	2.6	2.2–4.2	0		
	SUV _{mean}		1.8	1.8–3.3		1.8	1.8–3.3			
	MTV		1.4	1.1–1.8		1.4	1.1–1.8			
	TLA		3.2	2.0–4.6		3.2	2.0–4.6			

using iterative reconstruction and displayed on a PET/CT workstation (PET VCAR) in multiplanar reconstructions. Areas of focal tracer uptake were localized using the companion CT and classified as lesions of the breast, axillary nodes, or extraaxillary lesions. Three-dimensional regions of interest were placed in areas of tracer uptake, and measures of ¹⁸F-FDG avidity were recorded, including SUV_{max} (body weight), MTV (volume of tumor with SUV greater than 42% of SUV_{max}), SUV_{mean} (within the MTV), and total lesion glycolysis (TLG = MTV × SUV_{mean}).

Verification of Malignancy

All patients had biopsy-proven primary breast malignancy before enrollment in the clinical trial. Pathology for axillary nodes was also available for all patients. Pathologic evaluation of extraaxillary nodes was also available for the 3 patients with suspicious extraaxillary findings on ¹⁸F-fluciclovine PET/CT.

Statistical Analysis

Descriptive statistics were calculated for patient characteristics and measures of ¹⁸F-FDG avidity. Measures of ¹⁸F-FDG avidity were descriptively compared for patients with IDC and ILC and graphically demonstrated using box plots. In those with ¹⁸F-FDG scans, agreement between ¹⁸F-fluciclovine and ¹⁸F-FDG was calculated using the concordance correlation coefficient along with 95% confidence intervals. The agreement was also graphically illustrated using scatterplots with the line of perfect concordance versus the empiric least-squares model line. All analyses were performed using SAS 9.4 (The SAS Institute) and R 3.1.2 with the “epiR” package (The R Foundation).

RESULTS

Twenty-seven female patients were prospectively accrued to the institutional review board–approved protocol and underwent ¹⁸F-fluciclovine PET/CT. The median age of the cohort was 52.7 y (range, 37.3–79.1 y). The histology of the primary breast malignancy was IDC in 19 patients (70%) and ILC in the remaining

8 patients (30%). ILC patients were actively sought for inclusion into the study, which accounts for the higher prevalence of ILC in our cohort than in the overall breast cancer population. Patient

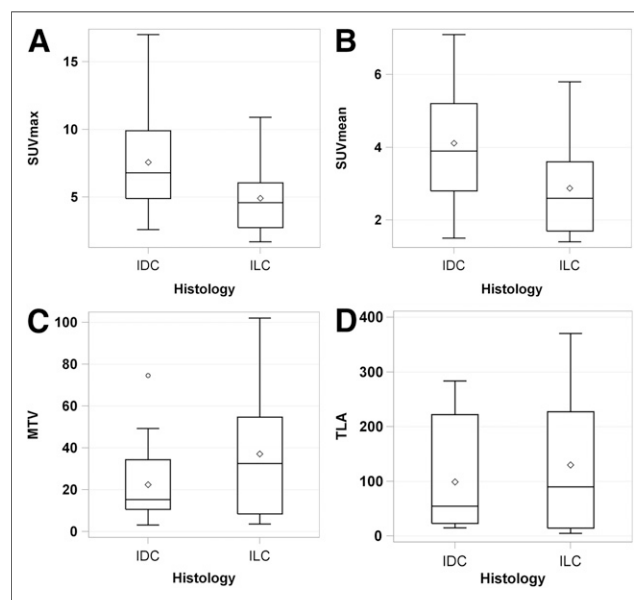


FIGURE 1. Distribution of measures of ¹⁸F-fluciclovine avidity in 27 primary breast malignancies. Tukey box and whisker plots are displayed for SUV_{max} (A), SUV_{mean} (B), MTV (C), and TLA (D) for IDC and ILC histologies. These plots are a schematic for distribution of values. Ends of box represent 25th and 75th percentiles (or first and third quartiles), whereas center line and diamond represent median and mean, respectively. 75th minus 25th percentile equals interquartile range, and ends of whiskers are placed at 1.5 times interquartile range. Any values lying outside these boundaries are considered outliers (for example, circle in MTV plot).

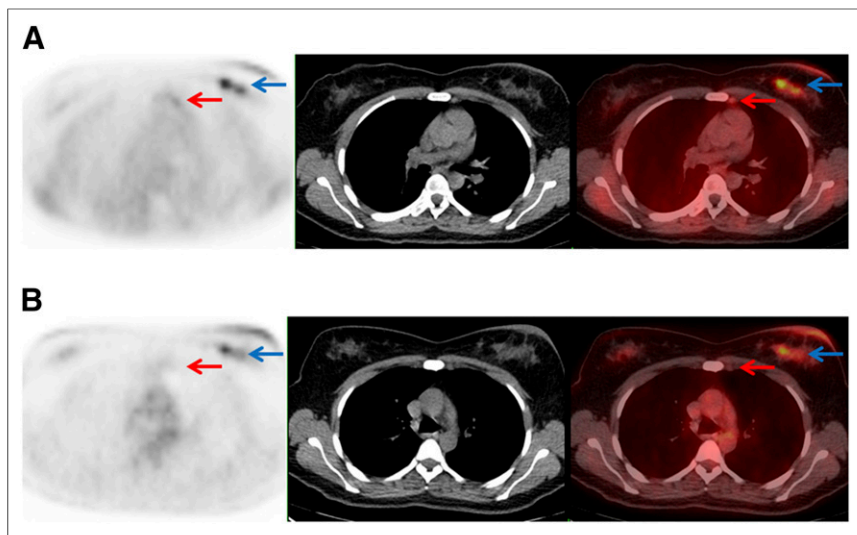


FIGURE 2. A 48-y-old woman with estrogen receptor–positive human epidermal growth factor receptor 2–negative IDC. (A) Axial ^{18}F -fluciclovine PET, CT, and fused ^{18}F -fluciclovine PET/CT demonstrating primary left breast malignancy (blue arrow; SUV_{max} , 7.5) and internal mammary nodal metastasis that was subsequently biopsy-proven (red arrow; SUV_{max} , 2.4). Axillary (SUV_{max} , 7.4) and supraclavicular (SUV_{max} , 4.2) nodal metastases were also detected (not shown). (B) Axial ^{18}F -FDG, CT, and fused ^{18}F -FDG PET/CT demonstrating primary left breast malignancy (blue arrow; SUV_{max} , 4.0) as well as axillary (SUV_{max} , 5.2) and supraclavicular (SUV_{max} , 2.8) nodal metastases (not shown); however, internal mammary nodal metastasis (red arrow; SUV_{max} , 0.7) was not appreciated on initial review of ^{18}F -FDG PET/CT.

and tumor characteristics are summarized in Table 1. All 27 patients underwent ^{18}F -fluciclovine PET/CT before initiation of therapy. Physiologic ^{18}F -fluciclovine uptake was seen in the liver, pancreas, and skeletal muscle, as previously reported (20). Uptake in presumably normal breast tissue was low in all patients, ranging from SUV_{max} 0.5 to 1.5. ^{18}F -fluciclovine–avid lesions were observed in the breast, axillary nodes, and extraaxillary nodes.

For the primary breast malignancies, all 27 locally advanced breast cancers were ^{18}F -fluciclovine–avid above local breast background. Median SUV_{max} was 5.9 (range, 1.7–17.0). Values for SUV_{max} , SUV_{mean} , MTV, and TLA of the primary breast malignancies for the entire cohort, as well as categorized by histology, are provided in Table 2. The distribution of these measures of ^{18}F -fluciclovine avidity is graphically depicted in Figure 1.

For axillary nodal metastases, 21 of 27 patients had pathologically proven axillary nodal metastases, including 16 of 19 patients with IDC and 5 of 8 patients with ILC. ^{18}F -fluciclovine PET/CT demonstrated axillary nodes that were ^{18}F -fluciclovine–avid above local background in 20 of 21 patients with pathologically proven axillary nodal metastases, including all 16 patients with IDC and 4 of 5 patients with ILC. There were no ^{18}F -fluciclovine–avid axillary nodes in patients without pathologically proven axillary nodal metastases. In patients with ^{18}F -fluciclovine–avid nodes, the number of nodes ranged from 0 to 10 (median, 2). Values for SUV_{max} , SUV_{mean} , MTV, and TLA of the axillary nodal metastases for the entire cohort, as well as categorized by histology, are provided in Table 2.

For extraaxillary nodal metastases, 3 of 27 patients had pathologically proven extraaxillary nodal metastases, and all 3 were patients with IDC. Two patients had unsuspected ^{18}F -fluciclovine–avid internal mammary nodes, which were subjected to fine-needle aspira-

tion, confirming malignancy in each case. An example of a patient with an internal mammary nodal metastasis first detected on ^{18}F -fluciclovine PET/CT is shown in Figure 2. A corresponding ^{18}F -FDG PET/CT scan, obtained before ^{18}F -fluciclovine PET/CT in this case, did not appreciate the internal mammary nodal metastasis. Values for SUV_{max} , SUV_{mean} , MTV, and TLA of the extraaxillary nodal metastases for the entire cohort, and by histology, are provided in Table 2. No distant metastases were detected on ^{18}F -fluciclovine PET/CT.

Of the 27 enrolled patients, 14 also underwent ^{18}F -FDG PET/CT as part of their standard clinical care before initiation of therapy, enabling a comparison of measures of ^{18}F -fluciclovine and ^{18}F -FDG avidity in lesions identified in these cases. Values for SUV_{max} , SUV_{mean} , MTV, and TLA/TLG of the primary breast malignancies, axillary nodes, and extraaxillary nodes for the 14 patients who underwent both PET/CT studies are provided in Table 3. For all 4 patients with ILC, ^{18}F -fluciclovine avidity was greater than ^{18}F -FDG avidity. An example of a patient with ILC with greater ^{18}F -fluciclovine avidity than ^{18}F -FDG avidity is shown in Figure 3. For

the 10 patients with IDC, ^{18}F -fluciclovine avidity was generally lower than ^{18}F -FDG avidity. ^{18}F -fluciclovine SUV_{max} ranged from 3.3 to 9.9 (median, 6.8), whereas ^{18}F -FDG avidity ranged from 3.3 to 43.5 (median, 10.0).

The concordance between ^{18}F -fluciclovine and ^{18}F -FDG was extremely weak for both SUV_{max} and SUV_{mean} (concordance correlation coefficient [CCC], 0.04 and 0.08, respectively; 95% confidence interval, -0.16 – 0.24 and -0.21 – 0.36 , respectively). However, the concordance between ^{18}F -FDG MTV and ^{18}F -fluciclovine MTV was strong (CCC, 0.89; 95% confidence interval, 0.73–0.96). The concordance between ^{18}F -FDG TLG and ^{18}F -fluciclovine TLA was moderate (CCC, 0.57; 95% confidence interval, 0.20–0.80). Concordance plots provide a graphical depiction of the data, as shown in Figure 4. If there was perfect concordance between ^{18}F -fluciclovine and ^{18}F -FDG, then the least-squares regression line would approach the line of perfect concordance, and the values would congregate around these lines. For example, the least-squares regression line for ^{18}F -fluciclovine MTV and ^{18}F -FDG MTV approaches the line of perfect concordance, demonstrating excellent concordance in the measurement of metabolic tumor volumes.

DISCUSSION

We hypothesized that the upregulation of amino acid transport proteins in breast cancer could favor enhanced ^{18}F -fluciclovine uptake and allow for clinically valuable imaging.

The results of the study tend to support the hypothesis but need to be confirmed in a larger series.

The locally advanced breast malignancies in this trial were all detected by ^{18}F -fluciclovine. The larger size of these primary malignancies aided detection, but the ability to detect

TABLE 3

Measurements of ¹⁸F-Fluciclovine and ¹⁸F-FDG Avidity in Primary Breast Malignancies, Axillary Nodes, and Extraaxillary Nodes of 14 Patients Who Underwent Both ¹⁸F-Fluciclovine PET/CT and ¹⁸F-FDG PET/CT

Lesion site	Measurements of avidity	By histology								
		All patients (n = 14)			IDC (n = 10)			ILC (n = 4)		
		n	Median	Minimum to maximum	n	Median	Minimum to maximum	n	Median	Minimum to maximum
¹⁸F-fluciclovine										
Breast malignancy	SUV _{max}	14	6.8	3.6–10.9	10	6.8	3.6–9.9	4	6.1	4.5–10.9
	SUV _{mean}		3.5	2.1–5.8		3.5	2.1–5.2		3.6	2.5–5.8
	MTV		18.2	3.2–102.0		14.2	3.2–74.6		54.7	34.7–102.0
	TLA		59.8	16.6–370.6		43.0	16.6–276.0		227	97.2–370.6
Axillary nodes	SUV _{max}	13	5.8	1.3–14.6	10	5.4	1.3–12.6	3	8.2	5.8–14.6
	SUV _{mean}		3.5	1.0–7.9		3.2	1.0–7.9		4.9	3.5–6.2
	MTV		5.2	1.0–22.1		5.2	1.0–13.4		4.1	2.2–22.1
	TLA		16.7	1.0–137.0		17.0	1.0–52.3		14.4	10.8–137.0
Extraaxillary nodes	SUV _{max}	2	3.4	2.6–4.2	2	3.4	2.6–4.2	0		
	SUV _{mean}		2.6	1.8–3.3		2.6	1.8–3.3			
	MTV		1.6	1.4–1.8		1.6	1.4–1.8			
	TLA		3.9	3.2–4.6		3.9	3.2–4.6			
¹⁸F-FDG										
Breast malignancy	SUV _{max}	14	6.2	1.8–43.5	10	10.0	3.3–43.5	4	3.7	1.8–6.0
	SUV _{mean}		3.7	1.6–15.1		4.5	2.4–15.1		2.4	1.6–3.6
	MTV		13.7	1.1–143.0		11.5	2.6–63.3		43.5	1.1–143.0
	TLG		62.4	1.9–673.5		49.7	6.2–673.5		148	1.9–228.8
Axillary nodes	SUV _{max}	13	6.3	2.8–13.3	10	6.4	3.2–13.3	3	6.3	2.8–9.0
	SUV _{mean}		3.9	1.8–6.9		4.2	1.8–6.9		3.9	2.2–5.6
	MTV		3.7	1.3–11.8		3.7	1.3–11.8		2.2	1.5–10.7
	TLG		13.0	3.3–71.8		17.2	3.7–71.8		8.6	3.3–59.9
Extraaxillary nodes	SUV _{max}	2	4.9	2.8–6.9	2	4.9	2.8–6.9	0		
	SUV _{mean}		2.8	2.1–3.5		2.8	2.1–3.5			
	MTV		2.0	1.5–2.4		2.0	1.5–2.4			
	TLG		5.1	5.0–5.3		5.1	5.0–5.3			

earlier stage breast cancer is unknown and requires additional investigation.

The ability of ¹⁸F-fluciclovine to detect axillary nodal metastases was also high in these patients with locally advanced malignancies. Detection of axillary metastases in earlier stage breast cancer requires further investigation. ¹⁸F-fluciclovine PET/CT detected internal mammary nodal metastases that were previously unsuspected. In this respect, it was similar to ¹⁸F-FDG PET/CT, which is proven to detect unsuspected extraaxillary nodal metastases in locally advanced breast malignancies (25). There was even 1 case in which ¹⁸F-fluciclovine PET/CT detected an internal mammary node, subsequently proven to be a metastasis, which was not detected on ¹⁸F-FDG PET/CT. The small sample size limits the significance of this finding.

No distant metastases were detected in this trial. The detection of distant metastases was limited by the restriction of imaging to include only the chest. ¹⁸F-fluciclovine has prominent physiologic hepatic uptake, which may make detection of liver metastases challenging, although lung, brain, and bone lesions may be readily visible.

It is interesting to compare ¹⁸F-fluciclovine avidity and ¹⁸F-FDG avidity in these breast malignancies. The concordance for MTV was strong, suggesting that the tracers identify a similar volume of metabolically active tumor; however, the concordance for SUV_{max} was low, suggesting that the tracers indeed measure different metabolic processes within these tumors. This raises the possibility that different subtypes of breast cancer may favor uptake of different tracers. For example, of the 4 patients with ILC who underwent both ¹⁸F-fluciclovine and ¹⁸F-FDG scans, all demonstrated ¹⁸F-fluciclovine avidity greater than ¹⁸F-FDG avidity. Future studies will be needed to understand the concordance between ¹⁸F-fluciclovine and ¹⁸F-FDG in ILC patients.

The strength of this study is its design as a prospective clinical trial, which decreases study biases and allows continued follow-up of a well-defined cohort. Its obvious weakness is its small numbers. These preliminary results are encouraging, but larger studies will be needed to further evaluate the place of ¹⁸F-fluciclovine for the PET/CT imaging of breast cancer.

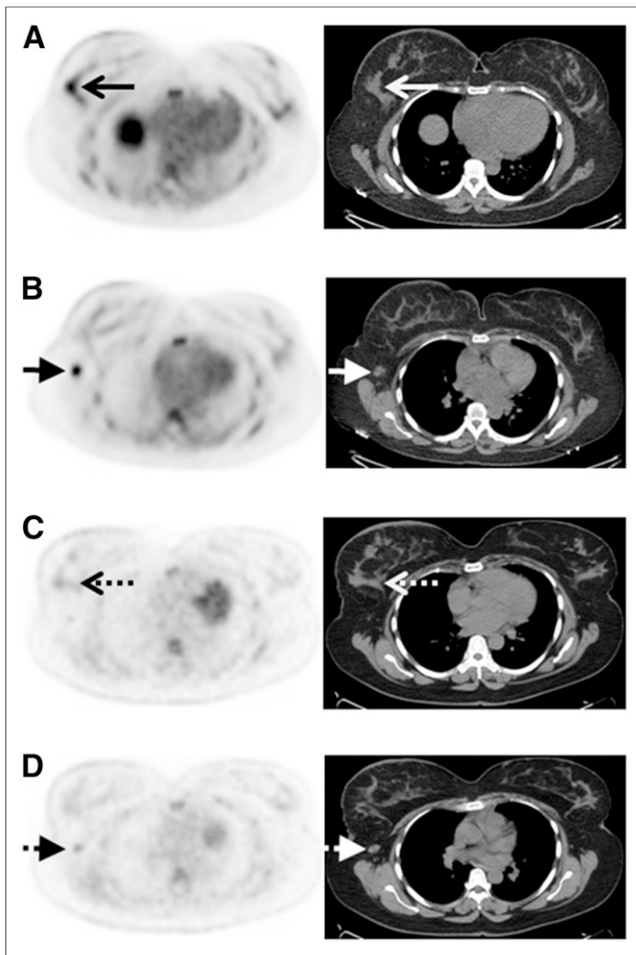


FIGURE 3. A 43-y-old woman with estrogen receptor-positive human epidermal growth factor receptor 2-negative ILC, which was more ^{18}F -fluciclovine-avid than ^{18}F -FDG-avid. (A) Axial ^{18}F -fluciclovine PET/CT demonstrates ^{18}F -fluciclovine-avid (SUV, 4.9) primary right breast malignancy (arrows). (B) Axial ^{18}F -fluciclovine PET/CT demonstrates ^{18}F -fluciclovine-avid (SUV, 5.8) right axillary nodal metastasis (short arrows). (C) Axial ^{18}F -FDG PET/CT demonstrates near background ^{18}F -FDG avidity (SUV, 1.8) in right breast malignancy (dashed arrows). (D) Axial ^{18}F -FDG PET/CT demonstrates only mild ^{18}F -FDG avidity (SUV, 2.8) in right axillary nodal metastasis (short dashed arrows).

CONCLUSION

^{18}F -fluciclovine PET/CT demonstrates potential for imaging of both IDC and ILC, including the detection of unsuspected extraaxillary nodal metastases. Uptake of the amino acid analog ^{18}F -fluciclovine does not parallel uptake of ^{18}F -FDG and thus provides a measure of a different metabolic process. ILCs were more ^{18}F -fluciclovine-avid than ^{18}F -FDG-avid, an observation that merits further study in a larger cohort.

DISCLOSURE

The costs of publication of this article were defrayed in part by the payment of page charges. Therefore, and solely to indicate this fact, this article is hereby marked “advertisement” in accordance with 18 USC section 1734. We acknowledge financial support from the Susan G. Komen for the Cure Research grant KG110441 (GAU) and GE Healthcare as well as support from the MSKCC

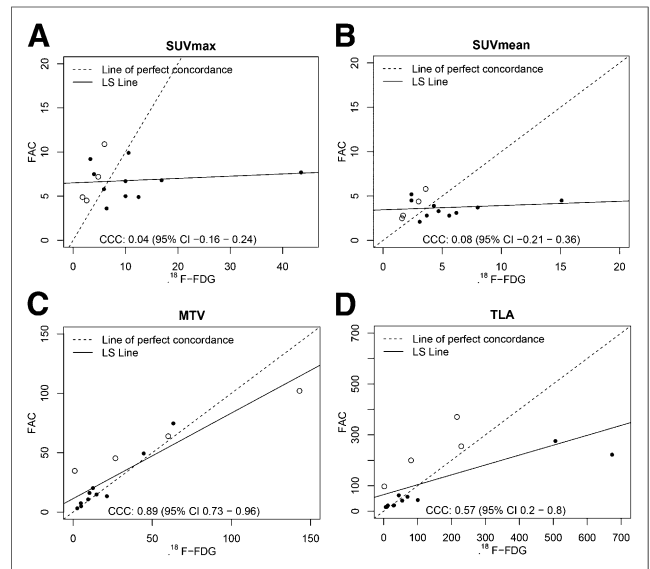


FIGURE 4. Concordance of ^{18}F -fluciclovine and ^{18}F -FDG SUV_{max} in 14 primary breast malignancies. Scatterplots for ^{18}F -fluciclovine versus ^{18}F -FDG, along with least-squares regression line (LS lines) and lines of perfect concordance, are displayed for SUV_{max} (A), SUV_{mean} (B), MTV (C), and TLA/TLG (D). Filled in circles represent IDC histology and open circles represent ILC histology. Line of perfect concordance represents condition in which ^{18}F -fluciclovine and ^{18}F -FDG values are exactly equal to each other. LS line represents fit of linear regression model for ^{18}F -FDG and ^{18}F -fluciclovine. Closer LS line is to line of perfect concordance, the stronger the agreement between ^{18}F -fluciclovine and ^{18}F -FDG values. CCC is measure of agreement between ^{18}F -fluciclovine and ^{18}F -FDG. It takes into account both correlation and accuracy between measurements. CCC values closer to zero are weak, and values closer to 1 are strong. $\text{FAC} = ^{18}\text{F}$ -fluciclovine.

Biostatistics Core and Radiochemistry & Molecular Imaging Probe Core (P30 CA008748) and the MSKCC Breast Cancer Research Fund. No other potential conflict of interest relevant to this article was reported.

ACKNOWLEDGMENTS

We thank Dr. Penny Ward from Blue Earth Diagnostics and Dr. Eugene Teoh from Oxford University for providing helpful comments on the manuscript.

REFERENCES

1. Groheux D, Espie M, Giacchetti S, Hindie E. Performance of FDG PET/CT in the clinical management of breast cancer. *Radiology*. 2013;266:388–405.
2. Kang BJ, Lee JH, Yoo Ie R, et al. Clinical significance of incidental finding of focal activity in the breast at ^{18}F -FDG PET/CT. *AJR*. 2011;197:341–347.
3. Fletcher JW, Djulbegovic B, Soares HP, et al. Recommendations on the use of ^{18}F -FDG PET in oncology. *J Nucl Med*. 2008;49:480–508.
4. Wahl RL, Siegel BA, Coleman RE, Gatsonis CG. Prospective multicenter study of axillary nodal staging by positron emission tomography in breast cancer: a report of the staging breast cancer with PET Study Group. *J Clin Oncol*. 2004;22:277–285.
5. Pearce R, Staff RT, Heys SD. The use of FDG-PET in assessing axillary lymph node status in breast cancer: a systematic review and meta-analysis of the literature. *Breast Cancer Res Treat*. 2010;123:281–290.
6. ECRI Evidence-Based Practice Center. *Effectiveness of Noninvasive Diagnostic Tests for Breast Abnormalities: Comparative Effectiveness Review No. 2* (prepared under contract 290-02-0019). Rockville, MD: Agency for Healthcare Research; 2006.

7. Riedl CC, Slobod E, Jochelson M, et al. Retrospective analysis of ¹⁸F-FDG PET/CT for staging asymptomatic breast cancer patients younger than 40 years. *J Nucl Med.* 2014;55:1578–1583.
8. Heudel P, Cimarelli S, Montella A, Bouteille C, Moggetti T. Value of PET-FDG in primary breast cancer based on histopathological and immunohistochemical prognostic factors. *Int J Clin Oncol.* 2010;15:588–593.
9. Berg WA, Gutierrez L, Ness-Aiver MS, et al. Diagnostic accuracy of mammography, clinical examination, US, and MR imaging in preoperative assessment of breast cancer. *Radiology.* 2004;233:830–849.
10. Lopez JK, Bassett LW. Invasive lobular carcinoma of the breast: spectrum of mammographic, US, and MR imaging findings. *Radiographics.* 2009;29:165–176.
11. Avril N, Rose CA, Schelling M, et al. Breast imaging with positron emission tomography and fluorine-18 fluorodeoxyglucose: use and limitations. *J Clin Oncol.* 2000;18:3495–3502.
12. Avril N, Menzel M, Dose J, et al. Glucose metabolism of breast cancer assessed by ¹⁸F-FDG PET: histologic and immunohistochemical tissue analysis. *J Nucl Med.* 2001;42:9–16.
13. Bos R, van Der Hoeven JJ, van Der Wall E, et al. Biologic correlates of ¹⁸fluorodeoxyglucose uptake in human breast cancer measured by positron emission tomography. *J Clin Oncol.* 2002;20:379–387.
14. Buck A, Schirrmeyer H, Kuhn T, et al. FDG uptake in breast cancer: correlation with biological and clinical prognostic parameters. *Eur J Nucl Med Mol Imaging.* 2002;29:1317–1323.
15. Dashevsky BZ, Goldman DA, Parsons M, et al. Appearance of untreated bone metastases from breast cancer on FDG PET/CT: importance of histologic subtype. *Eur J Nucl Med Mol Imaging.* 2015;42:1666–1673.
16. Hogan MP, Goldman D, Dashevsky B, et al. Value of ¹⁸F-FDG PET/CT for systemic staging of newly diagnosed invasive lobular breast cancer (ILC) as compared with invasive ductal breast cancer (IDC). *J Nucl Med.* 2015;56:1674–1680.
17. Osborne JR, Port E, Gonen M, et al. ¹⁸F-FDG PET of locally invasive breast cancer and association of estrogen receptor status with standardized uptake value: microarray and immunohistochemical analysis. *J Nucl Med.* 2010;51:543–550.
18. Shoup TM, Olson J, Hoffman JM, et al. Synthesis and evaluation of [¹⁸F]-1-amino-3-fluorocyclobutane-1-carboxylic acid to image brain tumors. *J Nucl Med.* 1999;40:331–338.
19. Amzat R, Taleghani P, Miller DL, et al. Pilot study of the utility of the synthetic PET amino-acid radiotracer anti-1-amino-3-[¹⁸F]fluorocyclobutane-1-carboxylic acid for the noninvasive imaging of pulmonary lesions. *Mol Imaging Biol.* 2013;15:633–643.
20. Schuster DM, Nanni C, Fanti S, et al. Anti-1-amino-3-¹⁸F-fluorocyclobutane-1-carboxylic acid: physiologic uptake patterns, incidental findings, and variants that may simulate disease. *J Nucl Med.* 2014;55:1986–1992.
21. Schuster DM, Nieh PT, Jani AB, et al. Anti-3-[¹⁸F]FACBC positron emission tomography-computerized tomography and ¹¹¹In-capromab pentetide single photon emission computerized tomography-computerized tomography for recurrent prostate carcinoma: results of a prospective clinical trial. *J Urol.* 2014;191:1446–1453.
22. Turkbey B, Mena E, Shih J, et al. Localized prostate cancer detection with ¹⁸F FACBC PET/CT: comparison with MR imaging and histopathologic analysis. *Radiology.* 2014;270:849–856.
23. Li CI, Uribe DJ, Daling JR. Clinical characteristics of different histologic types of breast cancer. *Br J Cancer.* 2005;93:1046–1052.
24. Svadberg A, Wickstrom T, Hjelstuen O. Degradation of acetonitrile in eluent solutions for [¹⁸F]fluoride PET chemistry: impact on radiosynthesis of [¹⁸F]FACBC and [¹⁸F]FDG. *J Labelled Comp Radiopharm.* 2012;55:97–102.
25. Fuster D, Duch J, Paredes P, et al. Preoperative staging of large primary breast cancer with [¹⁸F]fluorodeoxyglucose positron emission tomography/computed tomography compared with conventional imaging procedures. *J Clin Oncol.* 2008;26:4746–4751.
26. Edge S, Byrd D, Compton C. *AJCC Cancer Staging Manual.* 7th ed. New York, NY: Springer; 2010.